Study of entropy-driven self-assembly of rigid macromolecules

Issei Nakamura* and An-Chang Shi†
Department of Physics and Astronomy, McMaster University, 1280 Main Street West, Hamilton, Ontario, Canada L8S 4L8
(Received 8 April 2009; published 14 August 2009)

A simple model composed of two rigid macromolecules (adsorbents) immersed in a large number of small molecules (adsorbates) is used to study entropy-driven association processes. The surfaces of the adsorbents are capable of adsorbing the smaller adsorbates. The partition function of the model is obtained analytically. The probability of dimerization and the number of adsorbed molecules are shown to depend on the enthalpy and the entropy differences between the assembled and the disassembled states. Under certain conditions, dimerization of the macromolecules occurs with increasing temperature. This entropy-driven self-assembly is originated from an overall entropy gain due to the release of the adsorbed small molecules, leading to a large peak in the heat capacity due to the dimer formation. The desorption of the adsorbates induces a sharp change in the first-order derivative of the free energy, resulting in another large peak in the heat capacity. A temperature-induced re-entrance into the dimer state is also contained in the model.

DOI: 10.1103/PhysRevE.80.021112 PACS number(s): 05.20.−y, 64.75.Yz, 68.43.De, 81.16.Fg

I. INTRODUCTION

Molecular self-assembly or association is a generic phenomenon in physics, chemistry, and molecular biology. The driving force of the assembly is typically based on noncovalent intermolecular interactions such as hydrogen bonding and dispersion force [1–8]. Although this type of forces is weaker than covalent bonding, cooperative effects from a large number of molecules can often lead to thermally reversible macroscopic association and dissociation [9–11]. The thermal reversibility of molecular association is utilized in engineering functionalized single macromolecules (so-called supramolecules), which are capable of adsorbing smaller molecules. These supramolecules are also employed as chemical building blocks to form larger hierarchical structures [12]. The response to temperature stimulus has various potential applications such as drug delivery and polymerization in polar solvents.

The nature of the association processes can be discussed by considering the free-energy difference between the assembled and the disassembled states. In general, the free-energy difference can be expressed in terms of internal energy (enthalpy) and entropy differences, ΔE and ΔS, as $\Delta F = \Delta E - T\Delta S$. Here, we do not distinguish between the internal energy and the enthalpy because the volume of the system does not vary through the self-assembly [13]. Figure 1 shows ΔF as a function of temperature with the assumption of constant ΔE and ΔS (so-called van't Hoff equation [14]). The transition between the two states can be classified into two types, (a) and (b) [15,16]. In type (a), the assembled state is stabilized by attractive enthalpic interactions (i.e., enthalpy-driven association), $\Delta E < 0$. Dissociation occurs at high temperatures in order to gain the translational entropy. The enthalpy-driven association is characterized by the conditions $\Delta E < 0$ and $\Delta S < 0$. The second type, (b), corresponds to entropy-driven association. In contrast to type (a), the association arises with increasing temperature. It is obvious that the necessary conditions of entropy-driven assembly are $\Delta E > 0$ and $\Delta S > 0$.

In many experiments, molecular association has been observed when temperature is increased. That is, the association is driven by the entropy and the enthalpy increases. This entropy increase can often be traced to the release of adsorbed solvent molecules from the macromolecules. The self-assembly of tobacco mosaic virus and hepatitis B virus are two prominent examples exhibiting entropy-driven self-assembly [14]. The stability of the virus coat proteins has been studied using thermodynamical models [17,18]. Moreover, a generic thermodynamical model for the solvation of biopolymers is also proposed [19]. Another class of building blocks for entropy-driven assembly is found in synthetic macromolecules such as Rosette nanotubes (RNs) [20], zwitterion dimers [21], and supramolecular cages [22]. In contrast to the large accessible surface area of the globular protein or RNs, the zwitterion and the supramolecular cage have a relatively small number of hydrogen-bonding sites for the binding of solvent molecules. A further example of entropy-driven assembly is the crystallization of modified cyclodextrins [23]. In this system, crystallization occurs when the temperature is increased. The changes in the enthalpy and the entropy are obtained by the molar heat capacity curve in the differential scanning calorimetry (DSC) experiment [24]. The crystallization temperatures are estimated at 30 °C–90 °C from the peak of the curve.

Since the size of the adsorbents varies, the number of smaller molecules adsorbed on the surfaces of the macromolecules can be very different. Entropy-driven self-assembly of supramolecules can be found for different types of adsorbents and adsorbates, ranging from monomer-sized scale to protein-sized scale [21,25,26]. Thus, the association induced by the entropy gain should be considered as a generic phenomenon. In the literature, such an entropy-driven process is often analyzed using macroscopic models specifically designed for each experimental system. Although one can derive many useful results from the models, qualitative understandings on a microscopic level are often limited. Furthermore, mean-field approximations are also applied in

*nakamur@physics.mcmaster.ca
†shi@mcmaster.ca

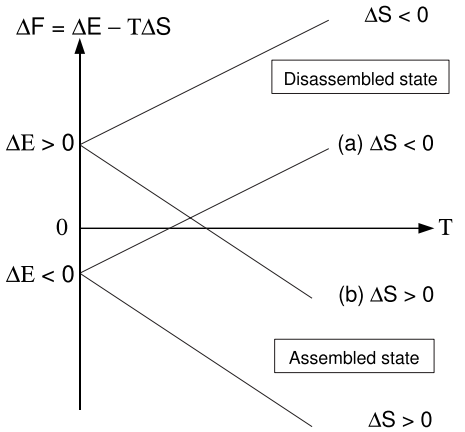

FIG. 1. Schematics of the free-energy difference between assembled and disassembled states. Note that the assembled state is energetically favorable when $\Delta F < 0$. (a) Enthalpy-driven transition. (b) Entropy-driven transition.

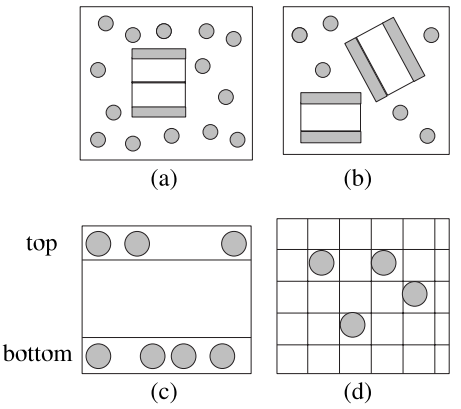

FIG. 2. Schematic description of the disassembly and the self-assembly of two rigid macromolecules (adsorbents) with smaller molecules (adsorbates). (a) The dimeric association with the "shell" of the adsorbed small molecules. (b) The dissociated macromolecules with the shell where n_i^t and n_i^b small molecules are adsorbed on the top and the bottom surfaces, respectively. (c) The side view of the macromolecule with the small molecules adsorbed on the surfaces. (d) The top view of the macromolecule with the small molecules on the adsorption sites. The adsorbates on the surfaces form a noninteracting ideal gas.

most of these models, where thermal fluctuations are ignored. From this perspective, exact solutions of statistical mechanics models will provide valuable insights into the nature of entropy-driven self-assembly.

In this paper, we propose a generic model with an explicit description of surface adsorption in order to gain a microscopic understanding of the entropy-driven self-assembly. The model may also provide guidance to experimental design of supramolecules. In Sec. II, we present a well-characterized statistical-mechanics model for the study of the entropy-driven dimerization of two rigid macromolecules (adsorbents). In this simple system, the small molecules are treated as noninteracting adsorbates. The surfaces of the macromolecules are capable of adsorbing the small molecules. In the model, the adsorbed molecules are allowed to move on the surfaces of the adsorbents, and hence they form a two-dimensional ideal gas on the surfaces. Although this model is a great simplification of real systems, it is expected that the model captures the qualitative nature of entropy-driven processes. The advantage of this model is that the partition function can be analytically obtained. This allows us to calculate thermodynamic properties such as the free energy and the heat capacity in Sec. III. Dimerization with increasing temperature arises from the release of the adsorbed small molecules. The association leads to a peak in the heat capacity, indicating a second-order-like phase transition. A sharp change in the first-order derivative of the free energy occurs with the desorption of the adsorbates, leading to a second peak in the heat capacity. The conditions for the spontaneous formation of the dimer are discussed in Sec. IV. In particular, a re-entrance into the dimer state with increasing temperature can be derived from the model.

II. PARTITION FUNCTION AND FREE ENERGY OF THE MODEL SYSTEM

The model is composed of two rigid macromolecules and N_w small molecules contained in a volume V_{tot}. As illustrated in Fig. 2, the small molecules can be adsorbed on the surfaces of the macromolecules. The two macromolecules are capable of forming a dimer with a specific binding interaction. The top and the bottom surfaces of the ith macromolecule have N_0 adsorption sites, which are occupied by n_i^t and n_i^b small molecules, respectively. These small molecules adopt different configurations on the adsorbing surfaces. Thus, the binomial coefficients, ${}_{N_0}C_{n_i^t}$ and ${}_{N_0}C_{n_i^b}$, enter the partition function. In addition, the mass of the small molecule, m_w, is assumed to be much smaller than the one of the macromolecule, m_h. Hence, the variation in the mass of the macromolecule for the uptake of the small molecules is ignored. The small molecule is a hard sphere with a volume v_w. Similarly, the volume of the macromolecule is v_h. The possible microstates are divided into two classes: the disassembled and the assembled states. The total partition function with two macromolecules and N_w small molecules is then given by

$$Z_{tot} = Z_{dis} + Z_{as}, \tag{1}$$

where Z_{dis} and Z_{as} are the partition functions of the disassembled and the assembled states,

$$Z_{dis} = \sum_{n_1^t=0}^{N_0} \sum_{n_1^b=0}^{N_0} \sum_{n_2^t=0}^{N_0} \sum_{n_2^b=0}^{N_0} \frac{{}_{N_0}C_{n_1^t} {}_{N_0}C_{n_1^b} {}_{N_0}C_{n_2^t} {}_{N_0}C_{n_2^b}}{2!\,(N_w - n_1^t - n_1^b - n_2^t - n_2^b)!} \times \int d\Omega_{dis} \exp\left[-\beta \left(-\varepsilon_{hw} n_1^t - \varepsilon_{hw} n_1^b - \varepsilon_{hw} n_2^t - \varepsilon_{hw} n_2^b + \frac{\vec{p}_{1h}^{\,2}}{2m_h} + \frac{\vec{p}_{2h}^{\,2}}{2m_h} + \sum_{i=1}^{N_w - n_1^t - n_1^b - n_2^t - n_2^b} \frac{\vec{p}_{iw}^{\,2}}{2m_w} \right) \right], \tag{2}$$

$$Z_{as} = \sum_{n_1^t=0}^{N_0} \sum_{n_2^b=0}^{N_0} \frac{{}_{N_0}C_{n_1^t} {}_{N_0}C_{n_2^b}}{(N_w - n_1^t - n_2^b)!} \int d\Omega_{as} \times \exp\left[-\beta \left(-\varepsilon_{hw} n_1^t - \varepsilon_{hw} n_2^b + \frac{\vec{p}_h^2}{2(2m_h)} - \varepsilon_{hh} + \sum_{i=1}^{N_w - n_1^t - n_2^b} \frac{\vec{p}_{iw}^2}{2m_\omega} \right) \right]. \quad (3)$$

In these expressions, $\beta = 1/k_B T$. The momenta of the ith small molecule and macromolecule are $\vec{p}_{iw}$ and $\vec{p}_{ih}$. The integrations in the phase space for the two macrostates are specified by

$$d\Omega_{dis} = d^3x_1^{(w)} d^3x_2^{(w)} \cdots d^3x_{(N_w - n_1^t - n_1^b - n_2^t - n_2^b)}^{(w)} d^3p_1^{(w)} d^3p_2^{(w)} \cdots \times d^3p_{(N_w - n_1^t - n_1^b - n_2^t - n_2^b)}^{(w)} d^3x_1^{(h)} d^3p_1^{(h)} d^3x_2^{(h)} d^3p_2^{(h)}, \quad (4)$$

$$d\Omega_{as} = d^3x_1^{(w)} d^3x_2^{(w)} \cdots d^3x_{(N_w - n_1^t - n_2^b)}^{(w)} d^3p_1^{(w)} \times d^3p_2^{(w)} \cdots d^3p_{(N_w - n_1^t - n_2^b)}^{(w)} d^3x^{(h)} d^3p^{(h)}, \quad (5)$$

where the superscript distinguishes between the macromolecule and the small molecule and the subscript denotes the ith molecule. Note that the Planck constant is set to unity. In order to mimic a short-range attractive intermolecular force such as hydrogen bonding, the interaction between the macromolecules is described as $-\varepsilon_{hh} < 0$. Similarly, $-\varepsilon_{hw} < 0$ denotes the attractive interaction between the macromolecule and the small molecule. Here, the number of small molecules in the bulk is assumed to be larger than the number of adsorbed molecules. Therefore, the approximation, $\frac{1}{(N-n)!} \sim \frac{1}{N!} \exp[n \ln N]$ for $N \gg n$, is applied to the partition function. The integrals in Eqs. (2) and (3) lead to

$$Z_{dis} = \frac{Z_{dis}^{kinetic}}{N_w!} a^{3N_w/2} \left(1 + \exp\left[\beta\varepsilon_{hw} - \ln \frac{a^{3/2}}{N_w} \right] \right)^{4N_0}, \quad (6)$$

where $Z_{dis}^{kinetic} = (V_{eff}^2/2)(2m_h\pi/\beta)^3$, $V_{eff} \equiv V_{tot} - N_w v_w - 2v_h$, and $a \equiv 2m_w \pi V_{eff}^{2/3}/\beta$. Similarly, one can obtain the partition function of the assembled state as

$$Z_{as} = \frac{Z_{as}^{kinetic}}{N_w!} a^{3N_w/2} \exp[\beta\varepsilon_{hh}] \left(1 + \exp\left[\beta\varepsilon_{hw} - \ln \frac{a^{3/2}}{N_w} \right] \right)^{2N_0}, \quad (7)$$

where $Z_{as}^{kinetic} = V_{eff}(4m_h\pi/\beta)^{3/2}$.

At equilibrium, the system accesses to one of these two classes of macrostates, and then it may transfer to the other class [13]. Thus, there are well-defined free energies for each molecular-scale subsystem [27],

$$F_{as} = -\frac{1}{\beta} \ln Z_{as} \quad (8)$$

and

$$F_{dis} = -\frac{1}{\beta} \ln Z_{dis}. \quad (9)$$

The probability of the self-assembly of the dimer can now be calculated from these partition functions,

$$P_{as} = \frac{Z_{as}}{Z_{tot}} = \frac{1}{\frac{\exp[-\tilde{\beta}q]}{\tilde{\rho}\tilde{\beta}^{3/2}} \left(\exp\left[\tilde{\beta} - C_{solv} + \frac{3}{2} \ln \tilde{\beta} \right] + 1 \right)^{2N_0} + 1}, \quad (10)$$

where $q \equiv \varepsilon_{hh}/\varepsilon_{hw}$, $C_{solv} \equiv \ln[(2m_w\pi\varepsilon_{hw})^{3/2}\rho_w^{-1}]$, $\rho_w \equiv N_w/V_{eff}$, $\tilde{\beta} \equiv \beta\varepsilon_{hw}$, $\tilde{V}_{eff} \equiv V_{eff}(m_h\pi\varepsilon_{hw})^{3/2}$, and $\tilde{\rho} \equiv \frac{2}{\tilde{V}_{eff}}$ are the scaled parameters. The adsorption energy ε_{hw} is set as a reference energy. The scaled temperature is given by $\tilde{T} = 1/\tilde{\beta}$. C_{solv} and $\tilde{\rho}$ are the scaled concentrations of small molecules and macromolecules, respectively. q denotes the scaled attractive interaction between the macromolecules. When q is larger than 1, the attractive interaction exceeds the binding interaction between the macromolecule and the small molecule. The difference of the scaled free energy between the dimerized and the dissociated macromolecules can be obtained as

$$\Delta F_{as} = \frac{F_{as} - F_{dis}}{\varepsilon_{hw}} = -q - \frac{1}{\tilde{\beta}} \ln \tilde{\rho} - \frac{3}{2\tilde{\beta}} \ln \tilde{\beta} + \frac{2N_0}{\tilde{\beta}} \times \ln\left(1 + \exp\left[\tilde{\beta} - C_{solv} + \frac{3}{2} \ln \tilde{\beta} \right] \right). \quad (11)$$

The scaled enthalpy difference $\Delta E(\tilde{T})$ is given by $\Delta E(\tilde{T}) = -\frac{\partial}{\partial\tilde{\beta}} \ln Z_{as} + \frac{\partial}{\partial\tilde{\beta}} \ln Z_{dis} = \Delta F_{as} + \tilde{T}\Delta S(\tilde{T})$, where $\Delta S(\tilde{T}) \equiv -\partial\Delta F_{as}/\partial\tilde{T}$ is the scaled entropy difference. Thus, $\Delta S(\tilde{T})$ is obtained by the slope of the tangent of ΔF_{as} at a given temperature $\tilde{T}$. The y intercept of the tangent at $\tilde{T}=0$ gives $\Delta E(\tilde{T})$.

To quantify the self-assembly induced by the release of the small molecules, the thermodynamic average of the number of adsorbed molecules, n_{ad}, is calculated. It follows from Eqs. (1), (6), and (7) that

$$n_{ad} = \frac{1}{\beta} \frac{\partial \ln Z_{tot}}{\partial \varepsilon_{hw}} = \frac{2N_0}{(1 + \tilde{\beta}^{-3/2} \exp[-\tilde{\beta} + C_{solv}])} \times \left[1 + \frac{1}{1 + \exp[\tilde{\beta}q]\tilde{\rho}\tilde{\beta}^{3/2}(1 + \tilde{\beta}^{3/2}\exp[\tilde{\beta} - C_{solv}])^{-2N_0}} \right]. \quad (12)$$

Hence, n_{ad} (adsorption number) is proportional to the number of adsorption sites on the surfaces. At the high-temperature limit, $\tilde{\beta} \to 0$, $n_{ad} \to 0$ is obtained. This result in-

dicates that the adsorbed molecules are thermally excited and released from the surfaces to the bulk phase. On the other hand, the low-temperature limit, $\tilde{\beta}\to\infty$, leads to the following two cases: (a) $n_{ad}\to 4N_0$ with $q\leq 2N_0$. In this case, the dimer is dissociated into the two macromolecules. The surfaces are completely covered with the shells. Therefore, the coefficient 4 arises from the total number of surfaces in the model. (b) $n_{ad}\to 2N_0$ with $q>2N_0$. This indicates that the two macromolecules are associated into the dimer. All of the adsorption sites are occupied by the small molecules.

In general, a large variation or divergence in the heat capacity arises from the transition between macroscopic states [28]. Therefore, we calculate the heat capacity at a constant volume C_v in Sec. III. Probabilities of the dimeric association are then compared with C_v. In our definition, the heat capacity for the ideal gas of the small molecules, C_v^{ideal}, is subtracted from the total heat capacity of the system, C_v^{tot}. It leads to

$$C_v = C_v^{tot} - C_v^{ideal} = -T\frac{\partial^2 F_{tot}}{\partial T^2} - \left(-T\frac{\partial^2 F_{ideal}}{\partial T^2}\right), \quad (13)$$

where F_{ideal} is the free energy of the ideal gas. Hence, C_v serves as the heat capacity for the effect due to the surface-induced association with the adsorption.

Furthermore, the macromolecules are expected to self-assemble or disassemble at a critical temperature $\tilde{T}_c$ and a critical macromolecular concentration (CMC) $\tilde{\rho}_c$. At the critical association point, the association and the dissociation of the dimer occur with the same probability [13]

$$P_{as}^c = P_{dis}^c = \frac{1}{2}, \quad (14)$$

where P_{as}^c and P_{dis}^c are the probabilities of the dimerization and the dissociation of the dimer at $\tilde{T}_c$ and CMC, respectively. Equations (10) and (14) lead to

$$\tilde{\rho}_c = \frac{\exp[-\tilde{\beta}_c q]}{\tilde{\beta}_c^{3/2}}\left[1+\exp\left(\tilde{\beta}_c - C_{solv} + \frac{3}{2}\ln\tilde{\beta}_c\right)\right]^{2N_0}. \quad (15)$$

When $\tilde{\rho}$ is larger than $\tilde{\rho}_c$, the dimeric association is obtained with a large probability (i.e., $P_{as}\geq\frac{1}{2}$). Thus, CMC provides the boundary for the spontaneous formation of the dimer. The thermodynamic properties of the association will be discussed with respect to the concentration and the temperature in the following sections.

The transitions at $\tilde{T}_c$ in the thermodynamic limit, $N_0\to\infty$, may be analyzed using Eq. (11). However, it is complicated to obtain the analytical expression because $\tilde{T}_c$ depends on N_0 in a nonlinear fashion, as indicated by Eq. (15). Instead, we will discuss the nature of the transitions numerically in Sec. III.

III. PROBABILITY OF DIMERIZATION

In this section, the entropy-driven and the enthalpy-driven dimerizations are analyzed by comparing the thermodynamic properties as functions of temperature. For typical parameters, plots of the dimerization probability [Eq. (10)], the free-energy difference [Eq. (11)], the number of adsorbed molecules [Eq. (12)], and heat capacity [Eq. (13)] are shown in Figs. 3–6. One important parameter controlling the behavior of the model is the ratio between the dimer binding and the adsorption energies, $q=\varepsilon_{hh}/\varepsilon_{hw}$. For $q>1$, typical ther-

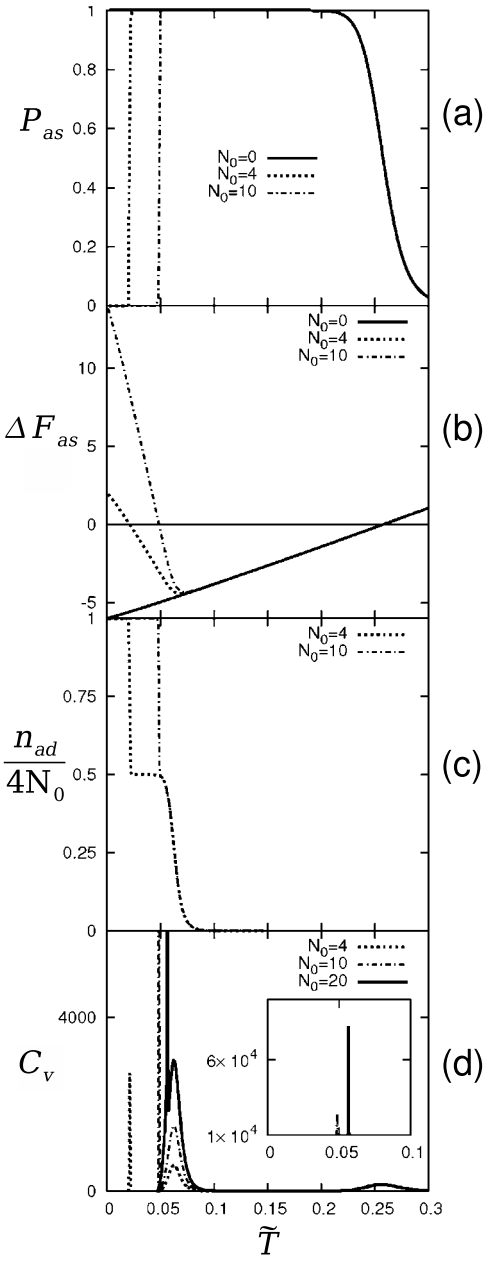

FIG. 3. (a) The probability of the dimerization. $P_{as}(\tilde{T}\to 0)\to 0$ with $2N_0>q$. (b) The difference of the free energy between the assembled and the disassembled states. The horizontal solid line denotes the zero axis. (c) The total number of small molecules adsorbed on the surfaces of the two macromolecules. (d) The heat capacity at a constant volume. The first spikelike peak arises from the entropy-driven association. The second relatively broad peak is due to the completion of the desorption. The complete dissociation of the dimer provides the third small bumpy peak. Note that, in all figures, $q=6$, $C_{solv}=20$, and $\tilde{\rho}=10^{-11}$ are used.

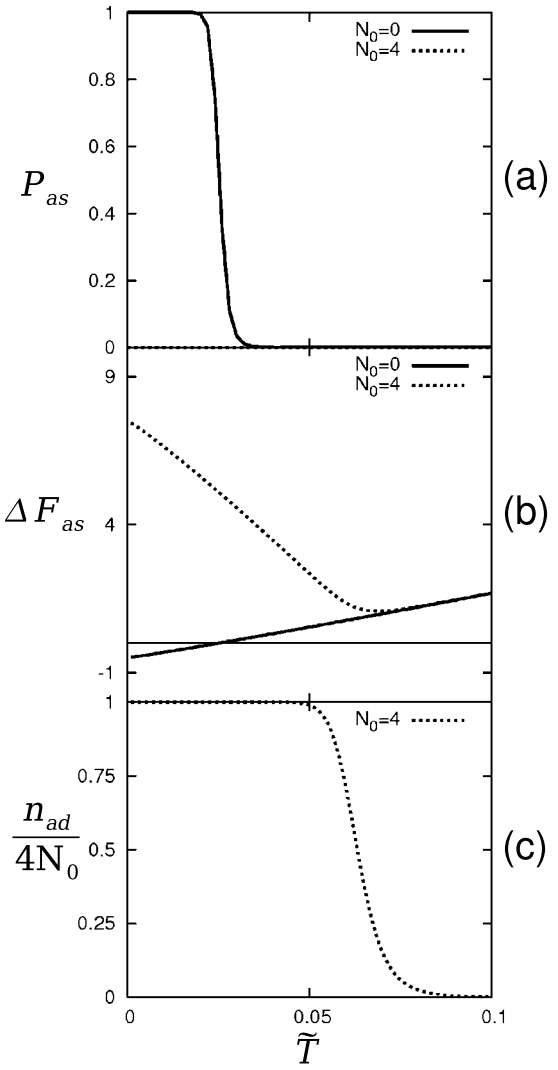

FIG. 4. (a) The probability of the dimerization. $P_{as}(\tilde{T}\to 0)\to 0$ with $2N_0 > q$. (b) The difference of the free energy between the assembled and the disassembled states. The horizontal solid line denotes the zero axis. (c) The total number of small molecules adsorbed on the surfaces of the two macromolecules. Note that, in all figures, $q=0.5$, $C_{solv}=20$, and $\tilde{\rho}=10^{-11}$ are used.

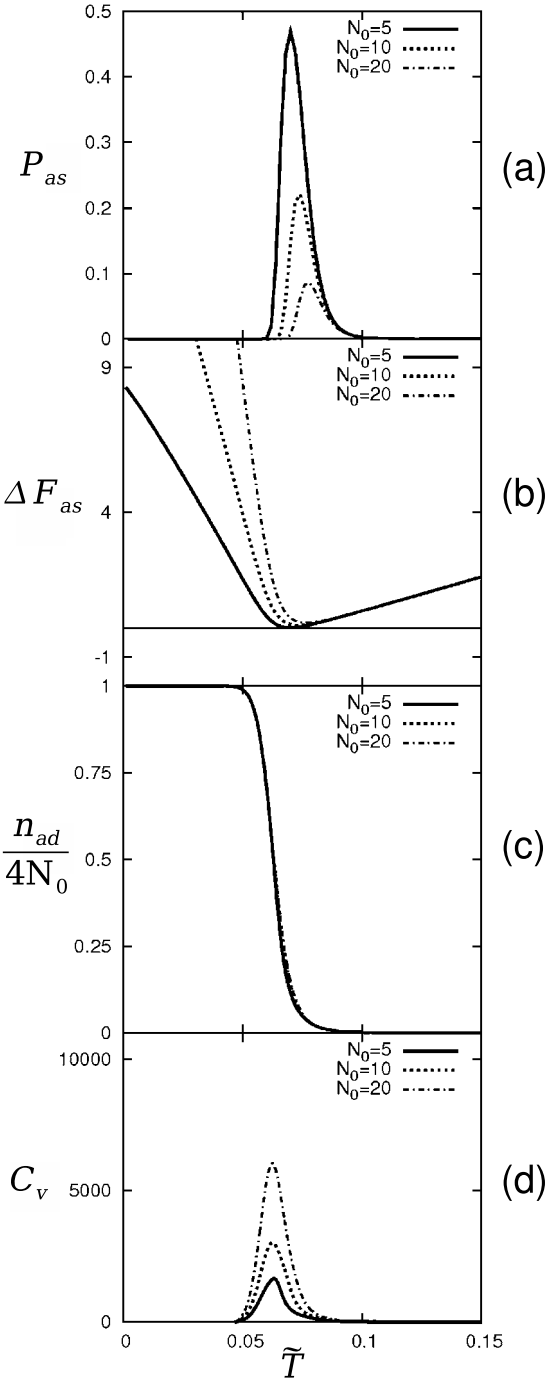

FIG. 5. (a) The probability of the dimerization. $P_{as}(\tilde{T}\to 0)\to 0$ with $2N_0 > q$. (b) The difference of the free energy between the assembled and the disassembled states. The horizontal solid line denotes the zero axis. (c) The total number of small molecules adsorbed on the surfaces of the two macromolecules. (d) The heat capacity at a constant volume. Note that, in all figures, $q=1.6$, $C_{solv}=20$, and $\tilde{\rho}=10^{-11}$ are used.

modynamic quantities are plotted in Fig. 3. In this case, the attractive interaction between the macromolecules is stronger than that between the macromolecule and the small molecule. For the special case of $N_0=0$, no small molecule can be adsorbed. In this case, the macromolecules can associate into the dimer at a low temperature. P_{as} starts from 1 at $\tilde{T}=0$. As the temperature is increased, P_{as} decreases to 0 monotonically, indicating that the dimer is dissociated at high temperature. This is a well-known behavior in statistical thermodynamics. In the case of $N_0 \neq 0$, the small molecules can be adsorbed on the surfaces of the macromolecules. When the energy of the disassembled state with the adsorption is lower than that of the assembled state, the dimer is dissociated into the two macromolecules at low temperatures. The condition of the low-temperature dissociation is given by $2N_0 \geq q$ (i.e., $-4N_0\varepsilon_{hw} \leq -2N_0\varepsilon_{hw} - \varepsilon_{hh}$). In this case, the two dashed lines for P_{as} approach 0 with $\tilde{T}\to 0$ in Fig. 3(a). However, as the temperature is increased, association occurs from the dissociated macromolecules, as shown by the large increase in P_{as}. The transition arises from an entropy gain by the release of small molecules from the surfaces. To elucidate the entropy-driven nature of this process, ΔF_{as} and n_{ad} as functions of temperature are shown in Figs.

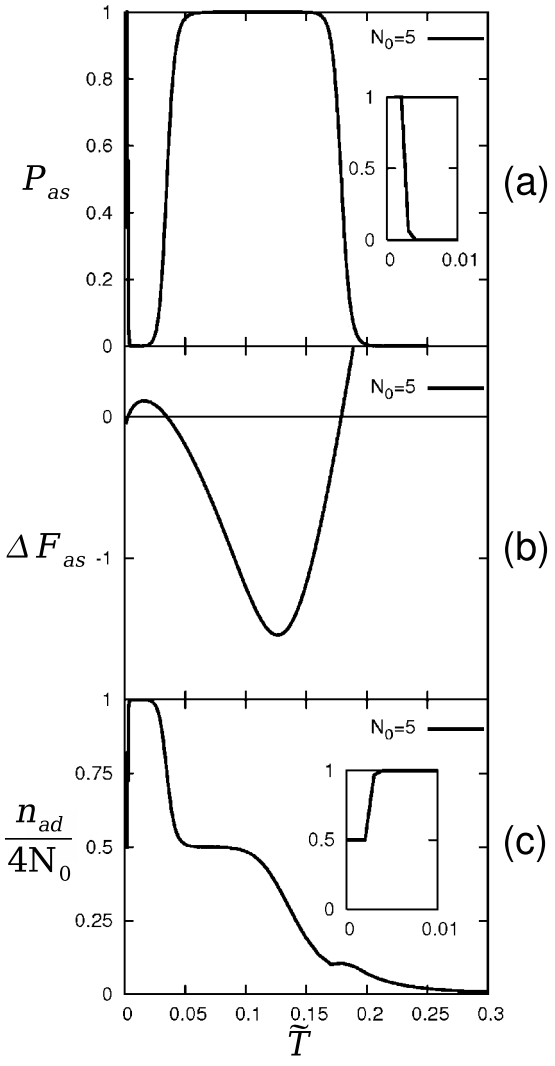

FIG. 6. (a) The probability of the dimerization. $P_{as}(\tilde{T}\to 0)\to 1$. (b) The difference of the free energy between the assembled and the disassembled states. The horizontal solid line denotes the zero axis. (c) The total number of small molecules adsorbed on the surfaces of the two macromolecules. Note that, in all figures, $q=10.1$, $C_{solv}=10$, and $\tilde{\rho}=10^{-25}$ are used.

3(b) and 3(c), respectively. When the large increase in P_{as} in Fig. 3(a) occurs with increasing temperature, $\Delta F_{as}<0$ is obtained. In this case, the tangent of ΔF_{as} has a negative slope and a positive y intercept, indicating that both entropy and enthalpy differences are positive. As discussed in Sec. II, the association is entropically driven. Figure 3(c) shows two regimes where there are two cascades of n_{ad}. n_{ad} sharply decreases to half of its original value through the first transition. Therefore, the increase in entropy is associated with a release of small molecules from the surfaces. Note that the surfaces of the dimer are still covered with small molecules in the first regime for the association because $n_{ad}\neq 0$ is obtained. Furthermore, Fig. 3(d) shows that the heat capacity exhibits three peaks with each set of the parameters. The first spikelike peak is at the temperature where the entropy-driven transition occurs. As N_0 is increased, a sharper peak appears and tends to diverge. Figure 3(b) shows that the slope of ΔF_{as} in this transition grows steeper with increasing N_0. This is due to a larger entropy difference between the two states. Therefore, the thermodynamic properties indicate that the entropy-driven association is a second-order phase transition at the thermodynamic limit, $N_0\to\infty$.

At a higher temperature, an abrupt change in the first derivative or slope of ΔF_{as} occurs. The "cusp" structure implies a first-order-like phase transition. The second cascade of n_{ad} appears in the proximity of this transition, where n_{ad} rapidly decreases to 0. Thus, this first-order-like phase transition is induced by the complete desorption of small molecules from the surfaces. In Fig. 3(d), the transition is also revealed as a second peak in C_v.

At temperatures above the complete desorption point, the dimer can still be stabilized by the attraction between the two macromolecules with $\Delta E<0$ and $\Delta S<0$. This dimerization is therefore an enthalpy-driven one. Dissociation occurs at a higher temperature with a relatively small peak in C_v. Note that this process is independent of N_0 because adsorbed small molecules are completely desorbed.

When the attraction between the macromolecules is weaker than the adsorption energy (i.e., $q<1$), the dimerization process is qualitatively different. Typical plots of the thermodynamic quantities in this case are shown in Fig. 4. It is apparent that the surface-induced cooperative transition does not occur with $q<1$ [Fig. 4(a)]. Figure 4(b) shows that the entropic effect does lead to a decrease in the free-energy difference ΔF_{as}. However, the dissociation of the macromolecules pre-empts the entropy-driven association, resulting in one single cascade of n_{ad} [Fig. 4(c)].

Figures 3 and 4 clearly show that the entropy-driven association is a result of the competition between the energy gain due to adsorption and the entropy gain due to desorption of the small molecules. This delicate competition is demonstrated in Fig. 5 for the case of moderate value of q ($q=1.6$) and large N_0. In this case, P_{as} has a sharp increase as the temperature is increased, similar to the steep increase shown in Fig. 3. This sharp increase is due to the desorption of the small molecules [Figs. 5(b) and 5(c)]. However, the dimerization process is interrupted by the dissociation of the dimers before P_{as} reaches a threshold value, $P_{as}^c=0.5$. The corresponding free energy ΔF_{as} is a decreasing function at low temperatures. Before reaching zero, ΔF_{as} makes a sharp turn to become an increasing function of $\tilde{T}$ [Fig. 5(c)]. Over the temperature range shown in Fig. 5, the dimer has higher free energy than the disassembled state. The system is thermally fluctuating between the ground state (two dissociated macromolecules) and the excited state (dimer). The sharp variation in the first derivative of ΔF_{as} occurs in close proximity to $\Delta F_{as}=0$. The entropy-driven excitation is accompanied by the completion of the desorption, and hence two cascades of n_{ad} are overlapped in Fig. 5(c). C_v in Fig. 5(d) exhibits a single large increase through the transition. Although a larger N_0 reduces the probability of the entropy-driven association in Fig. 5(a), the peak of C_v grows with increasing N_0. Therefore, the peak can be attributed to the desorption of small molecules, implying a first-order-like transition.

The competition between the energy and the entropy can lead to an entropy-driven re-entrance of dimerization, as

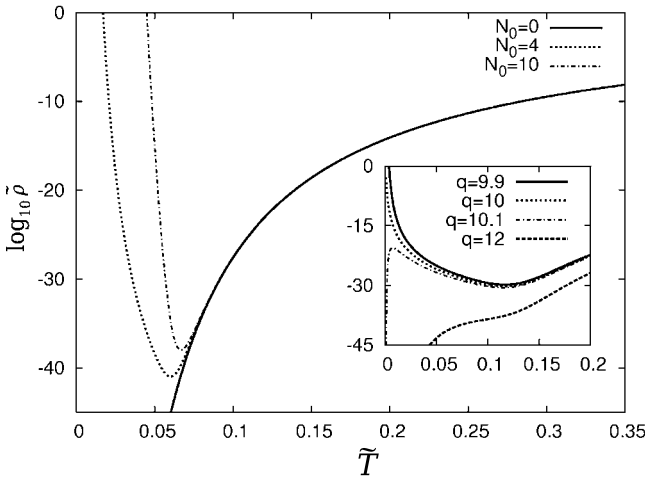

FIG. 7. The boundary of the transition between the associated and the dissociated states with $q=6$ and $C_{solv}=20$. Note that the y axis is $\log_{10}\tilde{\rho}$. The curves correspond to the CMCs determined by Eq. (15). The probability of the dimeric association is larger than 0.5 above the curves. At high temperatures, the line with $N_0\neq 0$ asymptotically approaches the one with $N_0=0$, since the dissociation of the dimer is not largely affected by the adsorption. The inset denotes the CMCs with $N_0=5$ and $C_{solv}=10$. The results indicate the temperature-induced re-entrance into the dimer state. The line with $q=12$ monotonically decreases with $\tilde{T}\to 0$.

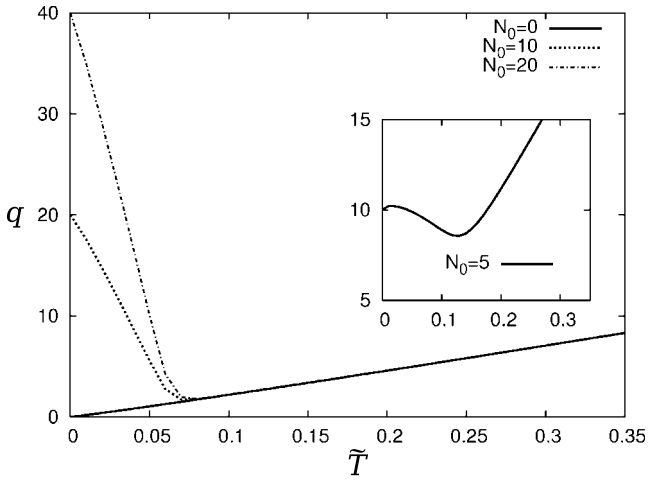

FIG. 8. The boundary of the transition between the associated and the dissociated states with the parameters used in Fig. 3 ($C_{solv}=20$ and $\tilde{\rho}=10^{-11}$). The curves are determined by Eq. (15). The probability of the dimeric association is larger than 0.5 above the curves. The inset denotes the phase diagram with the parameters used in Fig. 6 ($C_{solv}=10$ and $\tilde{\rho}=10^{-25}$). The result indicates the temperature-induced re-entrance into the dimer state.

shown in Fig. 6 for the case of large q ($q=10.1$). At very low temperature, the system is in the assembled state. As the temperature is increased, dissociation of the dimer occurs first. However, dimerization occurs again at a higher temperature ($\tilde{T}\sim 0.035$). From the free-energy plot shown in Fig. 6(b), it is clear that this re-entrance of the dimer state is driven by an entropy gain due to desorption of the small molecules [Fig. 6(c)].

IV. CMC

In this section, the dimer formation over a wide range of macromolecular concentration and temperature is analyzed using Eq. (15). The results are shown in Fig. 7, where the CMCs are plotted with different parameters. Since the region above the CMC curve has $P_{as}>0.5$, it is identified as the region of dimer state, whereas the lower region is the dissociated state. In the case of $N_0=0$, there is no entropy-driven force due to small molecules. Therefore, the dimer is straightforwardly dissociated as the temperature is increased. When there are adsorption sites on the surfaces, the entropy-driven association becomes possible. The macromolecules are, however, dissociated at sufficiently high temperatures. Furthermore, the re-entrance into the dimer state is indicated in the inset of Fig. 7. There are two critical points in this case, corresponding to the points at which $(\partial\widetilde{\rho_c}/\partial\widetilde{\beta_c})_{\widetilde{\beta_c^*}}=0$. The inset also shows that a larger value of q shifts the CMC to smaller values, resulting in a wider region of entropy-driven association. In other words, a stronger attractive force between the macromolecules enhances the stability of the entropy-driven state.

The CMC with a very large attraction between the macromolecules ($N_0=5$ and $q=12$) reveals that the region of entropy-driven dimerization disappears in this case. The asymptotic behavior of $\ln\widetilde{\rho_c}$ with $\widetilde{T_c}\to 0$ (or $\widetilde{\beta_c}\to\infty$) is given by

$$\ln\widetilde{\rho_c}|_{\widetilde{\beta_c}\to\infty}\sim(2N_0-q)\widetilde{\beta_c}+3\left(N_0-\tfrac{1}{2}\right)\ln\widetilde{\beta_c}. \qquad (16)$$

Therefore, when $2N_0\geq q$, $\ln\widetilde{\rho_c}$ monotonically increases to ∞ with $\widetilde{T_c}\to 0$. Entropy-driven dimerization is then expected to emerge in this case. As discussed in Sec. III, the condition implies that the dimer state is the excitation in energy level. Note that the temperature-induced re-entrance into the dimer state ($N_0=5$ and $q=10.1$) arises despite $2N_0\lesssim q$. The condition $2N_0\geq q$ is sufficient to provide entropy-driven dimerization, as illustrated in Fig. 7.

V. DISCUSSION AND CONCLUSION

In this paper, entropy-driven association of two rigid macromolecules into a dimer is studied using a simple model. The surfaces of the macromolecules are capable of adsorbing small molecules. When the model is extended to liquid systems with intermolecular interactions such as Lennard-Jones potential, the surface layer may resemble a solvation shell [19].

For all set of parameters of the model, the dimer is dissociated into the two macromolecules at a melting temperature T_m. On the other hand, it is possible that association is induced with increasing temperature below T_m. This is due to a gain of entropy by the release of the small molecules from the surfaces to the bulk phase. Moreover, a temperature-induced re-entrance into the dimer state is obtained from the model. In this case, two critical points appear in the phase diagram. The transitions in the model are summarized as phase diagrams in the q-T plane (Fig. 8).

The model exhibits second-order-like and first-order-like phase transitions which are due to entropy-driven association and the completion of the desorption of the small molecules, respectively. These transitions lead to peaks in the heat capacity, which tend to diverge with increasing N_0. The CMC indicates that entropy-driven dimerization occurs when $2N_0 \geq q$ (i.e., $-4N_0\varepsilon_{hw} \leq -2N_0\varepsilon_{hw} - \varepsilon_{hh}$). This condition implies that the dimer state covered with small molecules is an excited state in energy level. Thus, the entropy-driven transition is a thermal excitation of the two macromolecules.

When reasonable values of the model parameters are used, the entropy-driven association is predicted to occur at a temperature in the range, 0 °C–200 °C. For example, the parameters $N_0=4$, $\rho_w=100$ mM, $2/V_{eff}=0.1$ mM, $m_w=80$ g mol^{-1}, $m_h=150-150\,000$ g mol^{-1}, $\varepsilon_{hh}=20k_bT$, and $\varepsilon_{hw}=10k_bT$ lead to $T_c \sim 40$ °C. This is in good agreement with $T_c=30$ °C–90 °C for a hydrogen-bonded dimer in Ref. [21]. Hence, our simple model can be served as a qualitative description of the system. A good understanding of entropy-driven self-assembly due to the release of adsorbed molecules can be obtained from the model.

Before closing, it is appropriate to comment on the applicability of the simple model to realistic physical systems. For any macromolecules, conformational fluctuations are always present. The conformation difference before and after the assembly will contribute to the entropy difference, which should be included in the study of the assembling process. In the simple model employed in the current study, the conformation change of the macromolecules is ignored, so that the model system is analytically solvable. Qualitatively, the thermodynamic properties from the current model can serve as a guidance for the understanding of entropically driven assembly. On the other hand, quantitative application of the model results should be restricted to those systems where the macromolecular conformations do not change appreciably before and after the assembly. Examples of such rigid macromolecules could include virus coat proteins, Rosette nanotubes, cyclodextrins, and rodlike polymers.

Finally we would like to remark that our model can be extended to flexible polymeric systems, in which the conformational entropy of the polymers is included in the study. Furthermore, adsorption equilibrium could correlate with local monomer concentrations in this case. For example, the overlap of binding sites may occur through conformational changes of the polymers. Recently, we have shown that it is possible to develop a self-consistent field theory for flexible polymers with specific binding interactions and we intend to present this study in a future publication.

ACKNOWLEDGMENTS

This work was supported by the Natural Science and Engineering Research Council of Canada (NSERC).

[1] D. T. Bong, T. D. Clark, J. R. Granja, and M. R. Ghadiri, Angew. Chem., Int. Ed. **40**, 988 (2001).
[2] J. A. A. W. Elemans, A. E. Rowan, and R. J. M. Nolte, J. Mater. Chem. **13**, 2661 (2003).
[3] K. Harata, Chem. Rev. (Washington, D.C.) **98**, 1803 (1998).
[4] D. H. Williams and M. S. Westwell, Chem. Soc. Rev. **27**, 57 (1998).
[5] J. D. Hartgerink, E. R. Zubarev, and S. I. Stupp, Curr. Opin. Solid State Mater. Sci. **5**, 355 (2001).
[6] L. J. Prins, D. N. Reinhoudt, and P. Timmerman, Angew. Chem., Int. Ed. **40**, 2382 (2001).
[7] V. V. Yaminsky and E. A. Vogler, Curr. Opin. Colloid Interface Sci. **6**, 342 (2001).
[8] S. Otto and J. B. F. N. Engberts, Org. Biomol. Chem. **1**, 2809 (2003).
[9] T. Chen, M. H. Lamm, and S. C. Glotzer, J. Chem. Phys. **121**, 3919 (2004).
[10] K. Van Workum and J. F. Douglas, Phys. Rev. E **73**, 031502 (2006).
[11] D. Chandler, Nature (London) **437**, 640 (2005).
[12] S. C. Glotzer and M. J. Solomon, Nature Mater. **6**, 557 (2007).
[13] P. Nelson, *Biological Physics, Energy, Information, Life* (W. H. Freeman and Company, San Francisco, 2004).
[14] M. A. Lauffer, *Entropy-Driven Processes in Biology: Polymerization of Tobacco Mosaic Virus Protein and Similar Reactions* (Springer-Verlag, Berlin, 1974).
[15] D. M. Huang and D. Chandler, Proc. Natl. Acad. Sci. U.S.A. **97**, 8324 (2000).
[16] S. Rajamani, T. M. Truskett, and S. Garde, Proc. Natl. Acad. Sci. U.S.A. **102**, 9475 (2005).
[17] W. K. Kegel and P. van der Schoot, Biophys. J. **91**, 1501 (2006).
[18] W. K. Kegel and P. van der Schoot, Biophys. J. **86**, 3905 (2004).
[19] T. V. Chalikian, J. Phys. Chem. B **105**, 12566 (2001).
[20] H. Fenniri, B.-L. Deng, A. E. Ribbe, K. Hallenga, J. Jacob, and P. Thiyagarajan, Proc. Natl. Acad. Sci. U.S.A. **99**, 6487 (2002).
[21] C. Schmuck, Tetrahedron **57**, 3063 (2001).
[22] J. Kang and J. Rebek, Jr., Nature (London) **382**, 239 (1996).
[23] T. Aree, H. Hoier, B. Schulz, G. Reck, and W. Saenger, Angew. Chem., Int. Ed. **39**, 897 (2000).
[24] J. Frank, J. F. Holzwarth, and W. Saenger, Langmuir **18**, 5974 (2002).
[25] E. E. Dormidontova, Macromolecules **35**, 987 (2002).
[26] S. Bekiranov, R. Bruinsma, and P. Pincus, Phys. Rev. E **55**, 577 (1997).
[27] Note that, since $F_{tot}=-\frac{1}{\beta}\ln Z_{tot}=-\frac{1}{\beta}\ln(Z_{as}+Z_{dis})$, it follows that $F_{tot} \neq F_{as}+F_{dis}$.
[28] M. Plischke and B. Bergersen, *Equilibrium Statistical Physics*, 2nd ed. (World Scientific, Singapore, 1994).